Powder Technology 448 (2024) 120224

Contents lists available at ScienceDirect

Powder Technology

journal homepage: www.journals.elsevier.com/powder-technology

Development and process scaling of repeat mini-blending as a complementary approach to deliver continuous direct compression

Martin Prostredny [a], Hikaru Graeme Jolliffe [a], Richard Elkes [b], Khalid Maqsood [b], Yunfei Li Song [b], Gavin Reynolds [c], Bernhard Meir [d], John Robertson [a,*]

[a] CMAC, Technology and Innovation Centre, 99 George Street, Glasgow G1 1RD, UK
[b] GSK Ware R&D, Harris's Lane, Ware, Hertfordshire SG12 0GX, UK
[c] Oral Product Development, PT&D, Operations, AstraZeneca UK Limited, Charter Way, Macclesfield SK10 2NA, UK
[d] Gericke AG, Althardstrasse 120, CH-8105 Regensdorf, Switzerland

HIGHLIGHTS

- Equation for transferrable process conditions of a semi-batch Gericke Mini Blender.
- Demonstrated application to a low-dose formulation.
- Process intensification compared to traditional tumble blending.
- Rapid axial dispersion of components throughout the bulk of the powder.
- Limiting content uniformity based on particle size of active ingredient.

GRAPHICAL ABSTRACT

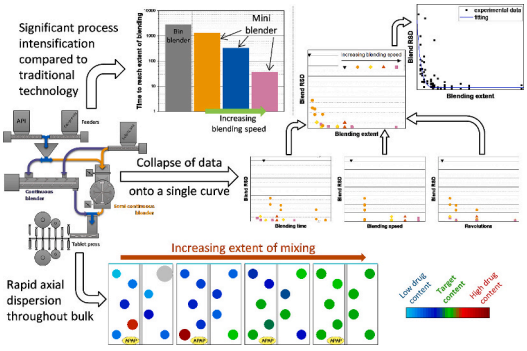

ARTICLE INFO

Keywords:
Powder blending
Continuous direct compression
Content uniformity
Axial dispersion
Process intensification

ABSTRACT

Process integration efforts in the pharmaceutical industry have led to an increased interest in Direct Compression, including Continuous Direct Compression. Accurate scale-up of powder blending and prediction of blend Critical Quality Attributes (CQAs) is key. The present work takes a modified approach for blend CQA characterisation in a high-shear semi-continuous blender (originally developed for low-shear batch blenders), and combines it with a blend content uniformity model (developed for high-shear continuous blenders) to characterise content uniformity responses of a high-shear semi-continuous blender (Gericke GBM-10-P Mini Blender).

Blend content uniformity assessed across process conditions and formulations shows that for a given formulation one set of model parameters can be regressed for all datapoints, allowing insight to be transferred between blender scales and types. This infers that lab-scale low-shear batch blenders can be used to predict the content

Abbreviations: APAP, Acetaminophen/paracetamol; API, active pharmaceutical ingredient; CDC, continuous direct compression; MCC, microcrystalline cellulose; HPLC, high-performance liquid chromatography; U.S. FDA, United States Food & Drug Administration.

* Corresponding author.
E-mail address: j.robertson@strath.ac.uk (J. Robertson).

https://doi.org/10.1016/j.powtec.2024.120224
Received 23 May 2024; Received in revised form 31 July 2024; Accepted 27 August 2024
Available online 28 August 2024

uniformity response of the high-shear semi-continuous blender, minimising materials consumption and experimental burden.

1. Introduction

Continuous, integrated and intensified manufacturing approaches have received substantial research interest in the pharmaceutical sector over the last decades [1,2], both for drug substance [3–5] and drug product [4,6–11], with some full end to end examples [4,12].

Within drug product manufacture, processes such as continuous granulation, roller compaction, and continuous direct compression (CDC) have been explored as routes for oral solid dose form manufacture [11]. A number of continuous drug product systems have been developed by manufacturers such as GEA, Glatt, Fette, Gericke, Lödige, and Hosokawa Micron [13–18] and implemented by industrial partners [7,19]. CDC is an attractive manufacturing route as it offers the simplicity in having only three core unit operations (feeding, blending, and compression) compared with granulation approaches, and also has reduced solvent and energy requirements (compared to wet granulation or hot melt extrusion) [20]. As a result of the perceived benefits of CDC, industrial partners are focussing greater efforts in this technology as a drug product process route for larger fractions of their development portfolios [21].

Whilst there are clear benefits of CDC, there are some key limitations of the technology, especially at early stages of development with regard to materials consumption [6,7,22]. During the product development stages (phase I to III), available Active Pharmaceutical Ingredient (API) quantities are very limited and the primary focus is to fully evaluate drug safety and efficacy leading to a need to ensure a lean drug product development pathway that will then seamlessly feed into robust long-term commercial production. Many of the CDC systems have blender hold up masses of some kilograms combined with the need to purge between steady states during process development and require the development of a complex disturbance monitoring, tracking and management strategy (via residence time distribution models and the use of process analytical technology) [6,23,24]. Therefore, full characterisation and validation of a CDC process is difficult until either sufficient quantities of materials are available or better predictive tools are developed.

The use of repeat semi-continuous blending systems such as the Mini Blender offered by Gericke, as a modular parallel alternative to a continuous blender in a CDC flowsheet (Fig. 1), may fill this gap and provide an opportunity for early development to launch activities, whilst providing the benefits of an integrated CDC process [25]; this is aligned with recent United States Food & Drug Administration regulatory guidelines on continuous manufacturing of drug substances and drug products [26]. At early stages, single or a small number of repeat mini blends can be made and as demand grows, repetitive cycles can be made in continuous-like operation to give increased flexibility and development simplicity at lower risk. A recent study by Jaspers and co-workers investigated the impact of material properties and process settings on critical quality attributes for CDC and exhibited intensification of the blending process, using the same blender type as the present work [27]. The authors presented a limited impact of material properties on variables such as blend uniformity, flowability, and tabletability using factorial regression analysis.

The evolution of a mixing process has been described using the decrease or decay in Relative Standard Deviation (RSD) for both batch and continuous blending [9,28]:

$$RSD(x) = \sqrt{RSD_{min}^2 + \left(RSD_0^2 - RSD_{min}^2\right)exp(-k_b x)} \quad (1)$$

where RSD_{min} is the minimum attainable RSD, RSD_0 is the theoretical RSD of an unblended mixture (the y-intercept), k_b is a sensitivity constant, and x is the independent variable (i.e. the x-axis). For batch tumble blending, time has been used for x [28], while strain has been used for a continuous system [9]. Both of these variables are related to the extent of mixing the powder has experienced at that point in time.

In the present work, a modified Kushner-Moore approach to blender performance characterisation is leveraged to define x in Eq. (1). Developed for tumbling batch blenders of various designs (such as IBC bin blenders, V-blenders, TURBULA® blenders), the Kushner-Moore approach is a transferable equation that allows, for a given formulation, the knowledge of how Critical Quality Attributes of blends – or tablets made from said blends – respond to blender operation [29–31]:

$$CQA = f(p_1, p_2 \ldots p_n, K) \quad (2)$$

where p_n are fitting parameters and K is a variable that represents the extent of mixing:

$$K = LFR \quad (3)$$

where, L is a characteristic mixing length scale (often taken to be the cube root of volume), F is headspace fraction (fraction of volume that is empty space i.e. can range from 0 to 1; bulk density is often used to determine headspace F), and R is the number of revolutions experienced by the material i.e. the product of blending speed (rotation rate) and time:

$$L = V^{\frac{1}{3}} \quad (4)$$

$$R = \nu t \quad (5)$$

where ν is rotation rate and t is time. An example of Eq. (2) where the CQA is tablet tensile strength σ is represented as follows [29–31]:

$$\sigma = \sigma_{\min} + (\sigma_{\max} - \sigma_{\min})exp\left(-\gamma V^{1/3} FR\right) \quad (6)$$

where $\sigma_{\min}$ is the lowest possible tensile strength of the formulation

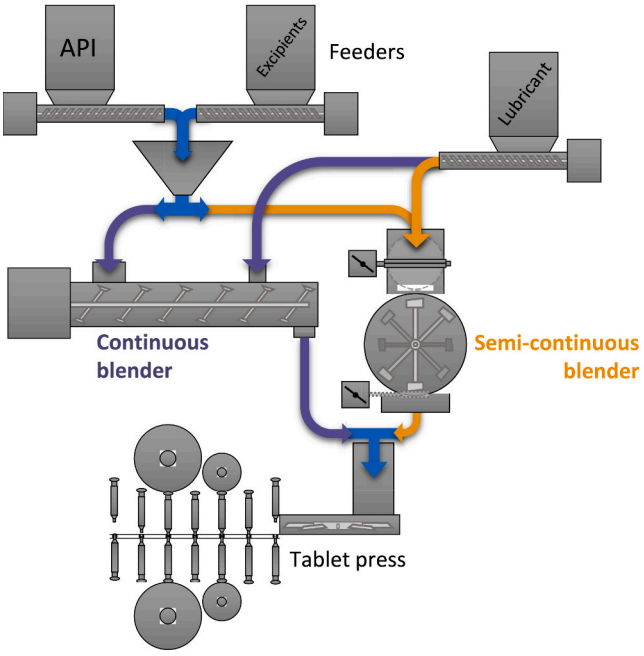

Fig. 1. Illustration of a semi-continuous blender (Gericke GBM 10-P Mini Blender) positioned as a parallel process alternative to a continuous blender within a CDC process.

(given fixed tablet press settings), σ_{max} is the theoretical tensile strength of an unblended formulation, γ is a formulation-specific sensitivity parameter. Authors of the present work previously reported that a modification to the approach of Eq. (1) (specifically concerning the response of tablet tensile strength i.e. a modification to Eq. 6) demonstrated that the inclusion of a Froude number term extends the approach to the semi-continuous Gericke Mini Blender (Fig. 1) [32]:

$$\sigma = \sigma_{min} + (\sigma_{max} - \sigma_{min})exp\left(-\gamma V^{1/3} FRFr^{n}\right), n = \begin{cases} 0 & if \quad Fr < 1 \\ 1/2 & if \quad Fr > 1 \end{cases} \tag{7}$$

or formulated more generally:

$$CQA = f(p_1, p_2 \ldots p_n, K') \tag{8}$$

$$K' = V^{1/3} \bullet F \bullet R \bullet Fr^{n}, n = \begin{cases} 0 & if \quad Fr < 1 \\ 1/2 & if \quad Fr > 1 \end{cases} \tag{9}$$

where Fr is the Froude number, the dimensionless ratio of inertial forces (that arise from rotation) to gravitational forces:

$$Fr = \frac{\left(\frac{2\pi v}{60}\right)^2 r}{g} \tag{10}$$

where r is the mixing radius, and g is the gravitational constant. Knowledge of Froude number is key, as typical tumbling batch blenders are restricted to Fr values below 0.4, while the Mini Blender – due its fundamentally different mode of operation of a static vessel with rotating blades – is capable of mixing at higher Fr values (in practical terms, at higher impeller speeds) [27,32,33].

In the present work, the work of Jaspers and co-workers [27] was expanded and the effect on the blend CQA of content uniformity (i.e. RSD) from extent of blending in the Gericke GBM 10-P Mini Blender characterised, that is to say Eq. (9) is used as the variable x in RSD Eq. (1), given that the former has been shown to be applicable for other CQAs:

$$RSD(x) = \sqrt{RSD_{min}^2 + \left(RSD_0^2 - RSD_{min}^2\right)exp\left(-k_b \bullet V^{1/3} \bullet F \bullet R \bullet Fr^{n}\right), n} = \begin{cases} 0 & \text{if} \quad Fr < 1 \\ 1/2 & \text{if} \quad Fr > 1 \end{cases} \tag{11}$$

2. Materials and methods

2.1. Materials

The blend formulations comprised a range of physical grades of paracetamol (APAP) as model API (micronised, mAPAP; powder, pAPAP; dense powder, dAPAP; special granular, sAPAP; and granular, gAPAP; sourced from Mallinckrodt, U.S.A.). The micronised mAPAP grade was used in the majority of blends prepared, unless stated otherwise. The excipients, anhydrous lactose (SuperTab® 21 AN) and microcrystalline cellulose (Pharmacel® 102) were donated by DFE Pharma (Germany) to represent common direct compression filler and compression aid respectively. The blends used in this work were chosen to align with prior work [29–32] with the addition of APAP as a surrogate API. The material properties of the individual components are given in Table 1.

2.2. Methodology

2.2.1. Blend preparation

The blends prepared in this work used a fixed lactose to microcrystalline cellulose (MCC) mass ratio of 1:2 and either 1 or 10 wt% APAP, leading to 33 or 30 wt% lactose and 66 or 60 wt% MCC, respectively. Common physical properties of the component materials were measured and the data is included in Table 1.

The equipment used in this work was a GBM 10-P Mini Blender from

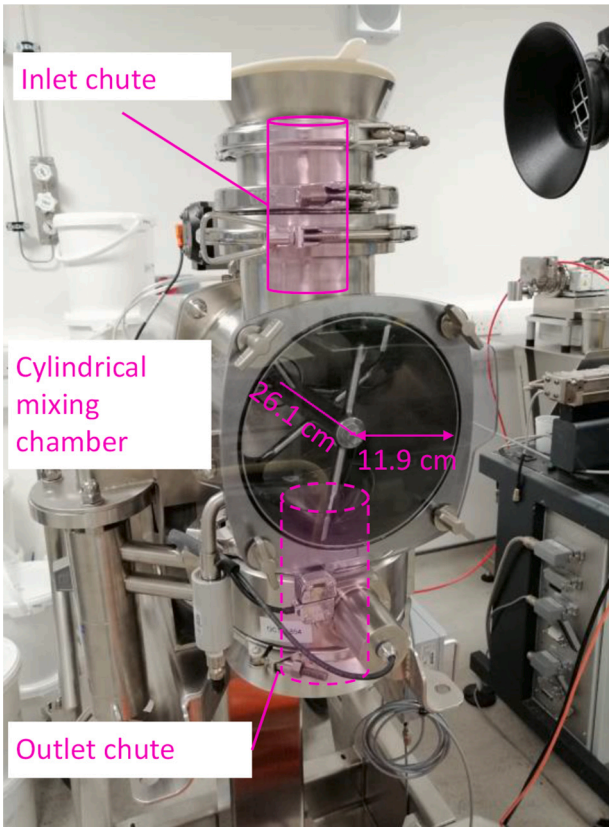

Fig. 2. The Gericke GBM 10-P Mini Blender. The mixing chamber is cylindrical (length 26.1 cm, radius 11.9 cm) with eight mixing paddles. Inlet and outlet chutes are vertical and feed/discharge via gravity (the latter assisted by several rotations of the blades at low speed).

Table 1
Physical properties of individual powder materials. Multiple grades of APAP have been used: micronised (mAPAP), powder (pAPAP), dense powder (dAPAP), special granular (sAPAP), and granular (gAPAP).

Compound	ρ_{bulk} (g/cm^3)	ρ_{tapped} (g/cm^3)	Carr's Index	Hausner ratio	ρ_{true} (g/cm^3)	d_{10} (μm)	d_{50} (μm)	d_{90} (μm)	$d_{[6,3]}$ (μm)
Pharmacel® 102	0.36	0.49	25.6	1.34	1.54	34	96	223	161
SuperTab® 21 AN	0.71	0.89	20.2	1.25	1.59	42	196	345	247
mAPAP	0.22	0.36	38.4	1.62	1.30	10	26	54	46
pAPAP	0.35	0.47	25.5	1.34	1.28	21	63	175	134
dAPAP	0.72	0.88	18.2	1.22	1.29	55	255	386	287
sAPAP	0.76	0.82	7.3	1.08	1.29	230	347	453	366
gAPAP	0.76	0.83	8.4	1.09	1.29	354	515	712	570

Gericke AG (Switzerland), a horizontal single-shaft mixer (Fig. 2); this is referred to as the Mini Blender in the present work. In order to avoid introducing additional differences between the experiments, materials were loaded into the Mini Blender in a fixed order of MCC, APAP, and lactose. The Mini Blender was loaded with the inlet valve manually open and the impeller static to avoid effects of any additional mixing in addition to the main blending process.

Blending regimes – and methods of mixing – vary according to RPM (more specifically, with Froude number, Eq. 10). A visual example is given in Fig. 3, where push mixing can be observed at 10 and 50 RPM, a transition to spin mixing has begun by 100 RPM with full spin mixing at 200 and 250 RPM, and centrifugal mixing at 300 RPM; for the majority of the experiments impeller speeds of 50, 100, 200, and 300 RPM were used to explore a range of mixing regimes (the maximum speed of the Gericke Mini Blender is 300 RPM). The various blending conditions (mass, speed, time, formulation) used to generate key results in the present work are tabulated in Table 2. Majority of blends were prepared using blend mass of 3 kg (corresponding to approx. 65 % volume fill), apart from the experiments exploring effects of fill level where the blend mass was revised to 2.25 and 3.75 kg. For selected conditions, blend mass values reduced to 0.5 kg were explored.

Composition, along with the blending conditions used, for each experimental run is included in the Supplementary Information (SI) in Section S2.

A single comparison mixture was prepared using a Pharmatech AB-015 tumble blender, as an example of commonly utilised batch blender. Total blend mass was kept at 3 kg and a 10 L bin was selected to mimic conditions in the Gericke Mini Blender. Blending speed was set to 20 RPM and the mixture was sampled for high-performance liquid chromatography (HPLC) analysis directly from the bin at times specified in Table 3 to span the wide range blending conditions used for the Mini Blender.

2.2.2. Sampling for HPLC analysis

Samples for APAP content analysis were collected here in two ways. For selected blends, samples were taken from the Mini Blender prior to discharge in order to analyse impact of blend discharge and transfer to storage vessel on blend uniformity. For sampling from the Mini Blender, 9 samples were taken from specific locations (Fig. 4). For the Pharmatech tumbling batch blender ten sampling locations throughout the IBC vessel were used (Fig. 5A).

Sampling procedure after discharge was performed for all the mixtures in this work using 10 spatially distributed sampling positions (Fig. 5B).

Each sample, for both pre- and post-discharge sampling, was taken from the corresponding bulk blend using a Sampling Systems Ltd. 12 mm powder thief (Part No. 1030 A-600) with a 1 mL volume tip (Part No. 1030AT-100) and transferred to a labelled glass vial. Average sample mass was ca. 500 mg, which is representative of a typical unit dose (tablet) mass. Samples collected in this manner were directly used for subsequent HPLC analysis, transferring and dissolving the whole amount of weighed powder for each sample. Details of the HPLC methodology are included in Section S1.2.

For axial dispersion study, discussed in Section 3.5, sampling from the Mini Blender was performed multiple times during the blending cycle with operation stopped at each time point, sampled as shown in Fig. 4 with operation subsequently resumed. The sampling times used for this part are presented in Table 4.

2.3. Blend uniformity limit estimation

To provide a reference value for best achievable RSD for the blends prepared here, a relationship from Hilden and co-workers is used, which assumes spherical API particles with known well-defined size and a randomly mixed powder blend [34]:

$$RSD_{ref} = \sqrt{\frac{\pi}{6} D^3_{[6,3]}} \times \sqrt{\frac{\rho_{API,true}}{m_{dose}}} \tag{12}$$

where $D_{[6,3]}$ is a weighted mean diameter (of the API) and $\rho_{\mathrm{API,true}}$ is the API true density; $D_{[6,3]}$ is readily reported in particle size analysers or can be calculated from typical particle size measurements such as d_{90}, and for additional detail on this variable the reader is referred to the work of Hilden and co-workers [34].

The relationship of Eq. (12) provides, for a given API dose m_{dose} (e.g.

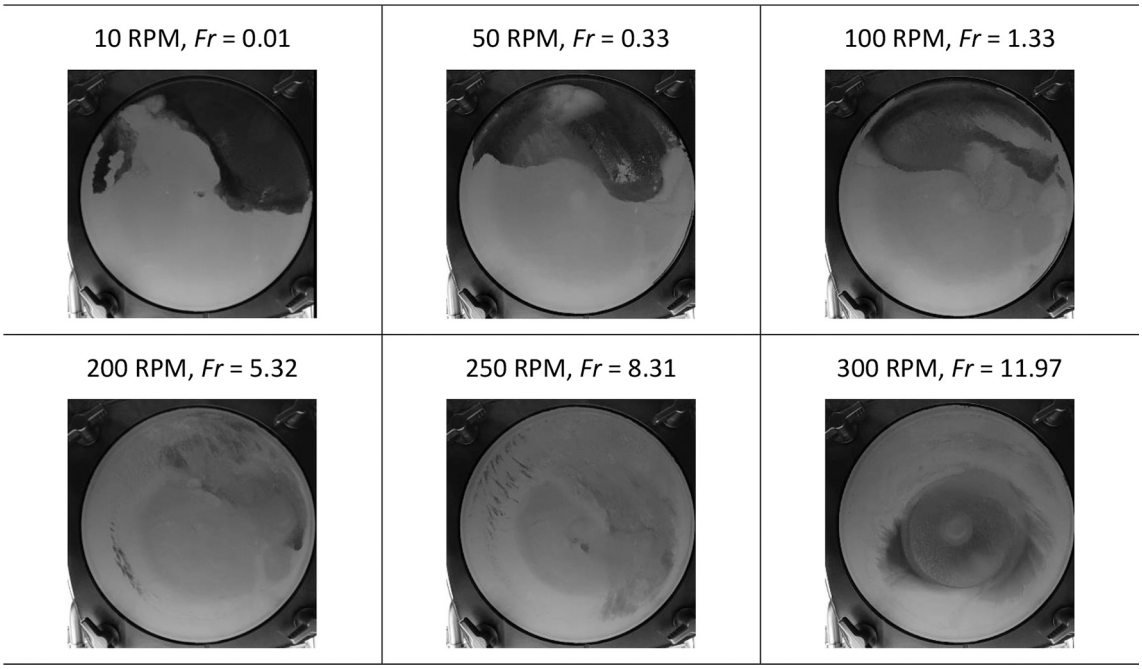

Fig. 3. Snapshots of Gericke Mini Blender with a at varying blender speed values, showing different blending regimes. Images extracted from high-speed video footage. Froude number *Fr* is calculated via Eq. (10). Powder used here is a 10 wt% pAPAP blend with balance being a 2:1 ratio of MCC (Pharmacel® 102) to lactose (SuperTab® 21 AN).

Table 2
Blending conditions used in the present work for the Gericke Mini Blender. The relevant sections of the present work's Results and Discussion are highlighted in the first column.

Section	Variable studied	Blending time (s)	Blending speed (RPM)	K' (Eq. 9) (dm)	API content (wt%)	Blend mass (kg)	API grade
3.1	blending time/speed	30–600	50–300	20–2740	10	3	mAPAP
3.2	API content	30–300	100–300	140–2740	1	3	mAPAP
3.4	blend mass	30–300	100–300	140–1370	1	0.5–3.75	mAPAP
3.5	axial dispersion				1	3	mAPAP
3.7	API physical grade	30–300	100–300	140–2740	1 & 10	3	pAPAP, dAPAP, sAPAP, gAPAP

Table 3
Composition and blending conditions for comparison bin blend prepared in Section 3.3.

Sampling step	Time (s)	Revolutions		K' (Eq. 9) (dm)	
1	180	60		9	
2	300	100		15	
3	1800	600		91	
4	3600	1200		181	
5	8400	2800		423	
6	26,400	8800		1328	
7	79,200	26,400		3985	
APAP		**Pharmacel® 102**		**SuperTab® 21 AN**	
Mass (g)	**Content (wt%)**	**Mass (g)**	**Content (wt%)**	**Mass (g)**	**Content (wt%)**
30.0	1.00	1980.4	66.00	990.0	33.00

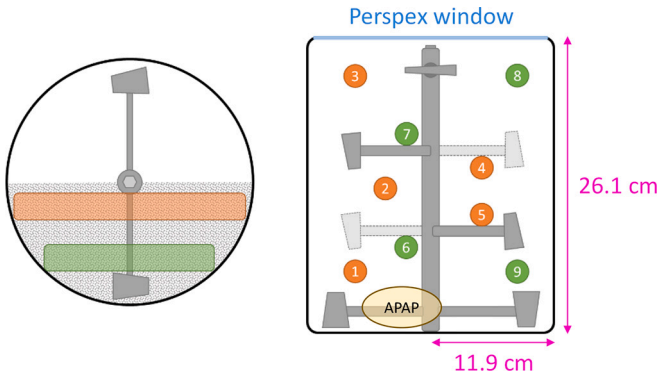

Fig. 4. Sampling locations from the Mini Blender before discharge, front view is shown on the left with top (orange) and bottom (green) layers for sampling and top view is presented on the right with the sampling locations colours corresponding to sampling layer, APAP loading location for axial dispersion experiments is shown in yellow. (For interpretation of the references to colour in this figure legend, the reader is referred to the web version of this article.)

a 500 mg sample of 10 % API would have an m_{dose} value of 50 mg), the lowest possible RSD for a material described by its true density $\rho_{API,true}$ and its particle size via $D_{[6,3]}$. The calculated values of best achievable RSD (assuming 500 mg average sample mass) for varying physical grades of APAP used in the present work are given in Table 5. Due to the lowest values of best achievable RSD for micronised APAP, this physical grade was used here for majority of experiments since this provides the widest window of blend uniformity and response to blending conditions.

3. Results and discussion

3.1. Blending time and speed scaling

Initially, blends with fixed composition and varied blending conditions were prepared, altering the blending speed and time values. A wide range of blending speed ν values between 50 and 300 RPM was used, along with blending times t up to 600 s, to achieve a different number of revolutions (50–1000 revolutions). In addition, selected values of number of revolutions were achieved using different blending speed and time values to better understand the effect of the experimental parameters on the resulting blend uniformity. Blend uniformity is represented here using the RSD of APAP content from HPLC analysis calculated from 10 samples. Lower RSD values correspond to increased APAP content uniformity, with smaller spatial variation of content within a mixture.

Plotting the data with blending time reveals a general trend of decreasing RSD with increasing time (Fig. 6a). The data also appears to be grouped by blending speed, with plateau RSD value reached at lower time values for higher blending speed, as would be expected.

Examining the data with respect to blending speed (Fig. 6b) presents a similar trend to Fig. 6a, where a wider spread along with higher RSD values is observed for lower speed values. Combining the blending speed and time into the number of revolutions experienced by the powder (Eq. 5) provides a clearer trend of decreasing RSD with the number of revolutions (Fig. 6c). There is still a relatively wide spread of values at lower number of revolutions with blending speed and the data can be seen grouped based on the blending speed.

Our previous work has involved using the same Mini Blender to investigate lubrication [32]. This included development of a lubrication scaling method with process conditions (Eq. 7), extending prior work by Kushner and co-workers [29–31]. The proposed lubrication scaling allows potential comparison with other blender technologies, as well as collapse of all mini blend lubrication data onto a single master curve to simplify process development. An analogy can be drawn between the process of lubrication and the process of blending of an active ingredient in a formulation. Both of these processes involve the dispersion and distribution of an ingredient in a bulk blend. In the context of lubrication, tablet tensile strength is used as a metric and with increased lubrication extent, this value reduces until reaching a plateau that is a function of the formulation [29–32]. In this study, APAP content RSD value (of a 500 mg sample) is used as the metric, which also decreases with increasing blending extent until reaching a plateau value that is a function of API particle size and sample size. Using this analogy, and considering that the same equipment was used, the same scaling was applied here and is discussed further below.

Further scaling of the x-axis with volume ($V = 11.59$ L), headspace fraction F, and Froude number Fr, is shown in Fig. 7; this is the approach used in our prior work (Eq. 7). While the present work uses one scale of Mini Blender (with a fixed volume) the term $V^{1/3}$ is kept to allow comparison with other blending technologies (such as the tumbling bin blender). This modified axis seems to collapse the data well onto a single curve, accounting for the combined effects of blending speed and time, as well as removes data clustering with speed observed with plotting against number of revolutions (Fig. 6). The data collapse suggests that the final blend RSD can be predicted by using the scaled x-axis of Eq. (*9*) (i.e. using Eq. *11*) and this accounts for the process route taken (i.e. combination of time and speed). It is important to note that the high RSD values at low extent of blending are associated with larger level of uncertainty, as these are more dependent on sampling from an inhomogeneous mixture.

Palmer and co-workers observed a similar trend of decreasing RSD with increasing value of strain, for a continuous system, until reaching a plateau [9]. This is similar to the trend obtained after scaling the data in

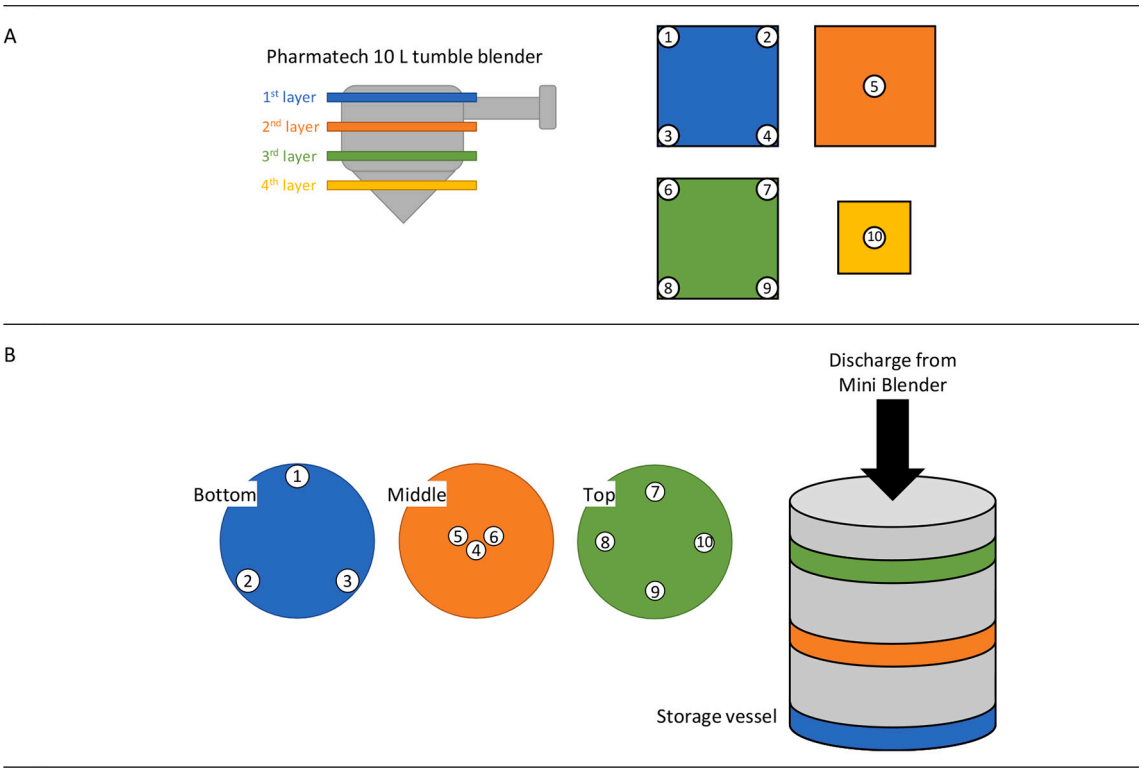

Fig. 5. Sampling locations for (A) Pharmatech tumbling bin blender and (B) blends after discharge from the Mini Blender. A 12 mm sample thief with 1 mL tip was used to extract samples from the numbered locations.

Table 4
Axial dispersion sampling.

Sampling No.	Revolutions	Time at 200 RPM (s)	Time at 100 RPM (s)
1	50	15	30
2	100	30	60
3	200	60	120
4	300	90	180
5	400	120	240
6	500	150	300

Table 5
Calculated values of best achievable RSD for varying physical grades and concentrations of APAP (Eq. 12). For the balance of the formulation (i.e. remaining 99 % or 90 %) was a 2:1 mix of MCC (Pharmacel® 102) to lactose (SuperTab® 21 AN). Sampling size of 500 mg.

API	RSD_{ref} for 1 wt% blend ($m_{dose} = 5$ mg)	RSD_{ref} for 10 wt% blend ($m_{dose} = 50$ mg)
mAPAP	0.4	0.1
pAPAP	1.8	0.6
dAPAP	5.7	1.8
sAPAP	8.1	2.6
gAPAP	15.8	5.0

this work. An analogy can be drawn between strain and the scaled x-axis as both are related to the extent of mixing the powder experiences during blending. However, for higher blending speed values that can be reached in the Mini Blender, the Froude number component needs to be considered [32].

3.2. Lower drug loading

The data, along with the scaling discussed above, was collected for 10 wt% APAP content. However, some high-potency compounds require much lower concentration of API. Therefore, blends with 1 wt% APAP, an order of magnitude lower than previously, were prepared in this section. Fig. 8 presents a comparison of the data for 1 and 10 wt% APAP blends and a similar trend can be observed for both concentrations, suggesting the same mixing mechanism is taking place. For 1 wt% content the best achievable RSD (Table 5) is slightly higher than for 10 wt% (0.4 % and 0.1 %, respectively) but both of these values are very low and beyond analytical limitations.

3.3. Comparison with traditional bin blending

Traditionally, low-shear tumble blending is often used to manufacture pharmaceutical blends. In order to provide a direct comparison with the Mini Blender investigated here, a 1 wt% APAP blend was prepared using a bin blender with the same total blend mass and similar internal volume. The bin blend was sampled at various time-points that align with the scaled data obtained for the Mini Blender (Fig. 9). The scaling used here collapses the data for both technologies on the same axis, allowing easier comparison.

The evolution of blend uniformity follows a similar pattern for both blending technologies, however, the time required to reach selected value of the scaled axis varies greatly (Fig. 10, visualised with select points used to show the difference). Below x-axis ca. 500 dm, relatively high RSD values are observed with insufficient mixing, with the region indicated in red. A shoulder can be identified around the value of 500 dm, where the data starts to reach a plateau (orange region in Fig. 10). Higher values of dm, above approx. 500–1000 dm, a plateau is reached with some variability between points but no further improvement of blend uniformity (green region in Fig. 10).

For the bin blender, since the Froude number (and therefore speed) is not effectively used for the scaling (due to *Fr* exponent $n = 0$ in Eq. *11*), the options to reach a given dm value in shorter time are limited. On the other hand, for the Mini Blender, increasing the blending speed can drastically reduce the time required to reach a selected value of dm. As

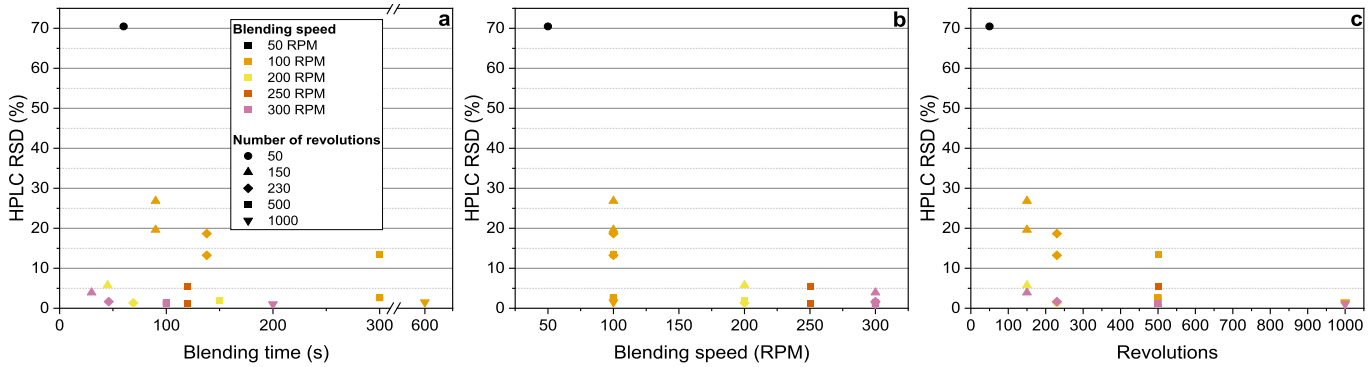

Fig. 6. APAP content RSD for 10 wt% blends with (a) blending time, (b) blending speed, and (c) number of revolutions, with blending speed indicated by colour and number of revolutions by shape of data points.

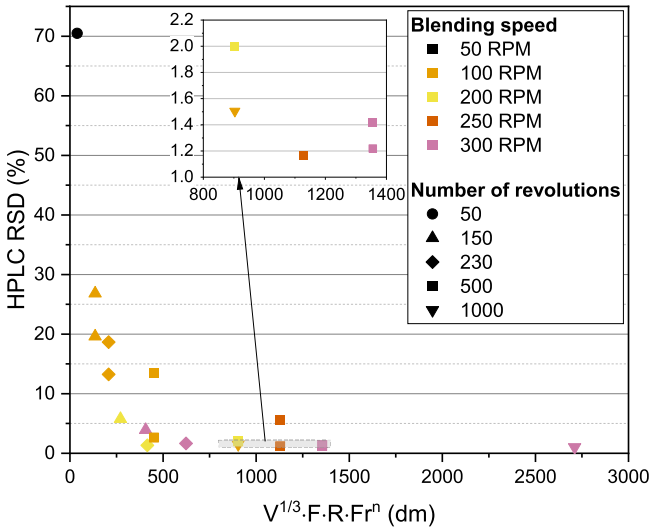

Fig. 7. APAP content RSD for 10 wt% blends with the scaled axis.

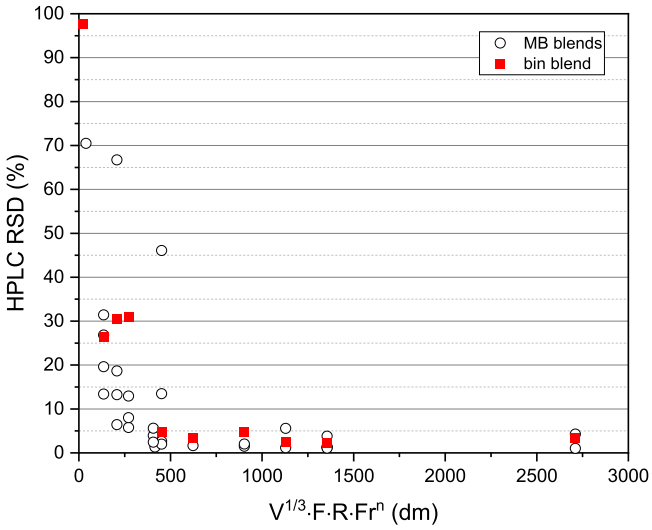

Fig. 9. Comparison of Mini Blender data (open circles; Table 2) and tumbling bin blender (red squares; Table 3). (For interpretation of the references to colour in this figure legend, the reader is referred to the web version of this article.)

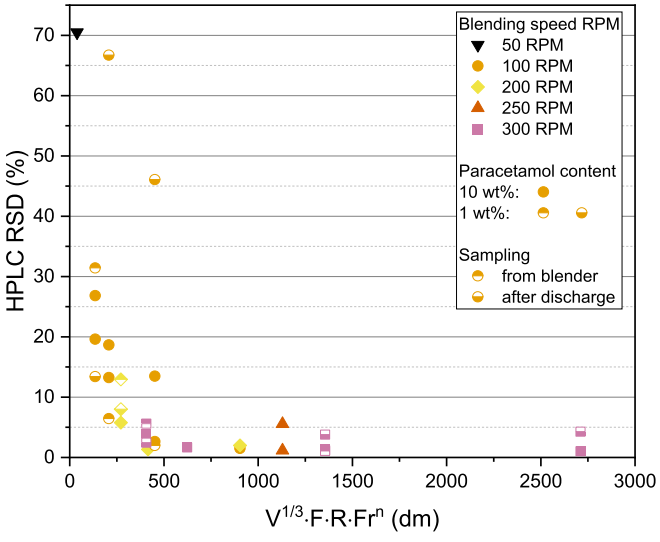

Fig. 8. APAP content RSD for 1 and 10 wt% blends with the scaled axis.

an example, to reach a value of 1000 dm (at the start of the plateau), using the bin blender would require almost 96 min. Using the Mini Blender, this time can be reduced to almost 44 min at 50 RPM, 11 min at 100 RPM, and only 73 s at 300 RPM, as illustrated in Fig. 10 for selected dm values. This offers a great opportunity for process intensification, providing up to 80-fold decrease in time required, compared to traditional tumbling technology. Thus, the use of a Mini Blender provides a meaningful solution for scale up in production without the associated risks of equipment change, as the same equipment would be used across production scales. Integrated in a semi-continuous line, assuming the 3 kg blend mass used in most of this study, a total throughput of 30 kg/h could be achieved with a cycle time of 6 min supporting continuous compression, whilst allowing sufficient time for material dispense, lubrication step, and discharge.

3.4. *Impact of blender fill level*

The importance of headspace in tumbling blenders, which impacts blending performance, is well recognized [31,32]. Depending on the process application, it might be beneficial to use higher blender fill levels (for instance, to increase process throughput) or lower ones (when only a limited amount of materials is available). In this study, the blend mass was varied from 3 kg (approx. 65 % volume fill) to 3.75 kg (ca. 82 % volume fill) and 2.25 kg (ca. 49 % volume fill) to explore the effects of fill level on blend uniformity. Furthermore, blend mass values as low as 0.5 kg (ca. 11 % volume fill) were also studied here to investigate the lower blend mass limit value. Photographs of the Mini Blender with varied level of blend mass are shown in Fig. 11.

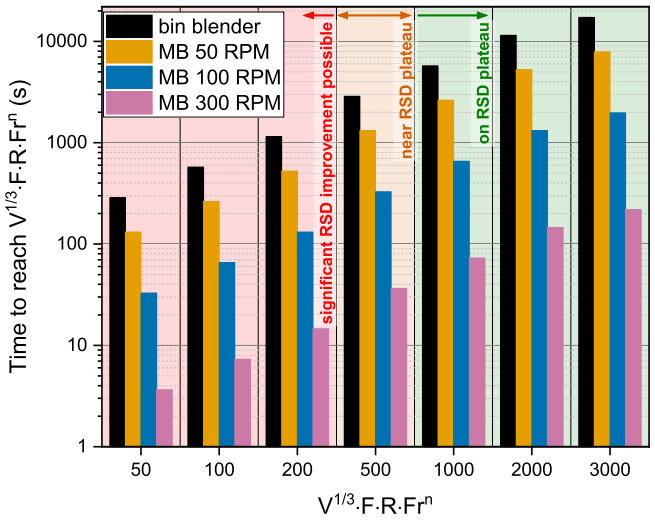

Fig. 10. Process intensification example comparing traditional bin blender technology and Mini Blender at various blending speed values, expected RSD value regions are shown in red (significant improvement of RSD may be possible by additional blending), orange (near RSD plateau value), and green (on RSD plateau, additional blending is not expected to improve blend uniformity). (For interpretation of the references to colour in this figure legend, the reader is referred to the web version of this article.)

Blend uniformity, represented as RSD values, is compared for the blends with varied total mass with the above data (Fig. 12). First, the data is scaled as in the previous sections (Fig. 12a) and the blends with varied blend mass follow a similar pattern as the main dataset for 3 kg mass. Since the original scaling relationship was developed for tumbling blenders, the data was scaled here also without including the headspace fraction F in the equation (Fig. 12b).

When the headspace fraction F is excluded from the scaling, datapoints for blends at the same blending conditions but different fill levels, which were previously spread out, now share the same x-axis value, e.g. the cluster around 4000 dm in Fig. 12b. It appears that the data is following a similar overall trend even without including the headspace fraction in the scaling. Therefore, it can be inferred that the Mini Blender fill level does not have a significant impact on the blend uniformity for a given set of blending conditions. For low-shear blenders, mixing occurs on the powder surface, the length of which is inversely proportional to fill level [29]. Increased values of F lead to a higher average number of avalanching events imparted upon the blend particles due to decreased blend perimeter. On the other hand, powder mixing in the Mini Blender occurs throughout the bulk as a result of the passing blades and therefore the resulting particle movement is not determined by the fill level. However, it should be noted that for comparison with low-shear blenders, a scaling factor with a value similar to the ones used here (F = 0.35 for 3 kg blend mass) needs to be included in order to align the blending extent axis.

Furthermore, the data shows that the total blend mass can be as low as 0.5 kg and still yield blend uniformity comparable to higher blender fill levels. This could be very useful during development work, where only a limited amount of API is available and this would allow processing using the same equipment from early (i.e. only a few batches are required) to late development stages (i.e. intense industrial scale process running with blend after blend, minimising waste and cycle times to achieve throughput). Based on the conclusions from this section, the blending extent for the Mini Blender, used to collapse the data, is defined as follows:

$$RSD(x) = \sqrt{RSD_{min}^2 + \left(RSD_0^2 - RSD_{min}^2\right) exp\left(-k_b \bullet V^{1/3} \bullet R \bullet Fr^n\right)}, n$$
$$= \begin{cases} 0 & \text{if } Fr < 1 \\ 1/2 & \text{if } Fr > 1 \end{cases} \quad (13)$$

3.5. Axial and radial dispersion

During the initial dispensing of individual components during a routine operation and/or integration with an automated feeding system, some of the API can end up in a relatively more difficult to reach areas of the blender, such as the corners. This could lead to a lower degree of uniformity at the end of the blending cycle, with a residual hotspot remaining in the original location. To examine powder dispersion, APAP was loaded in the back corner of the Mini Blender for the experiments in this section (as shown in Fig. 4). After set number of revolutions (Table 4), samples were taken from the blender, before the blending cycle was resumed.

Given that taking samples from the Mini Blender removes material for subsequent sampling at higher number of revolutions from the same blend, it is crucial to assess this impact. Using the approach above, 54 samples are taken from a blend in total. For a 1 wt% blend, assuming an average sample mass of 500 mg and an average content of 1 wt%, 0.27 g of the API is removed from the initial 30 g added for the 3 kg blend mass. This corresponds to only 0.9 %, a percentage that also applies to a 10 wt % blend. Consequently, the removal of material is not anticipated to significantly affect the data for subsequent sampling.

The visualisation of the APAP target concentration percentage for a selected example blend in Fig. 13 provides insight into the dispersion of the API throughout the blend volume during mixing. It is noteworthy that even after only 50 revolutions (Fig. 13a), the API is distributed

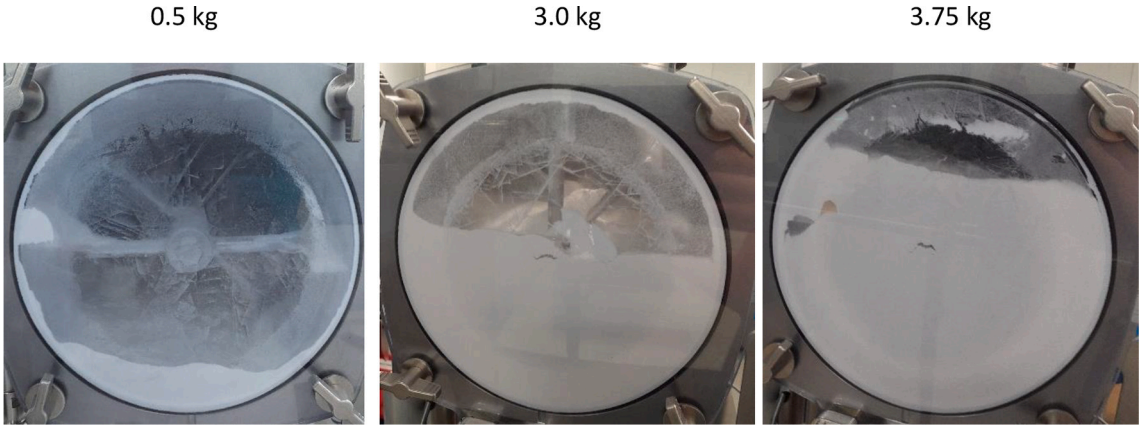

Fig. 11. Mini Blender fill level for 0.5 kg, 3.0 kg, and 3.75 kg blend mass.

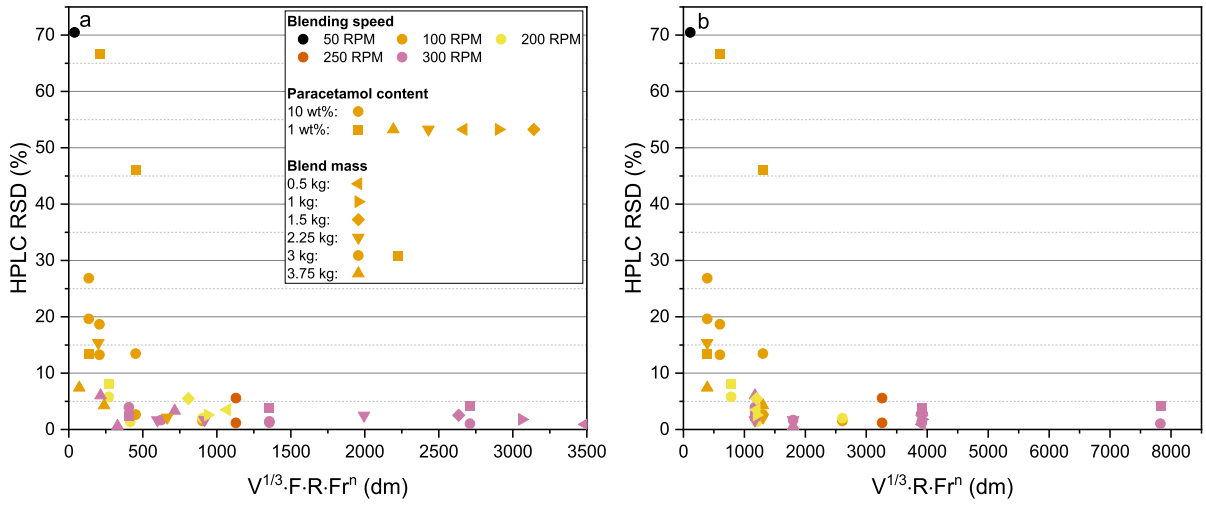

Fig. 12. APAP content RSD from HPLC analysis for varied fill level scaled (a) including and (b) excluding the headspace fraction F (i.e. Eqs. 11 and 13, respectively).

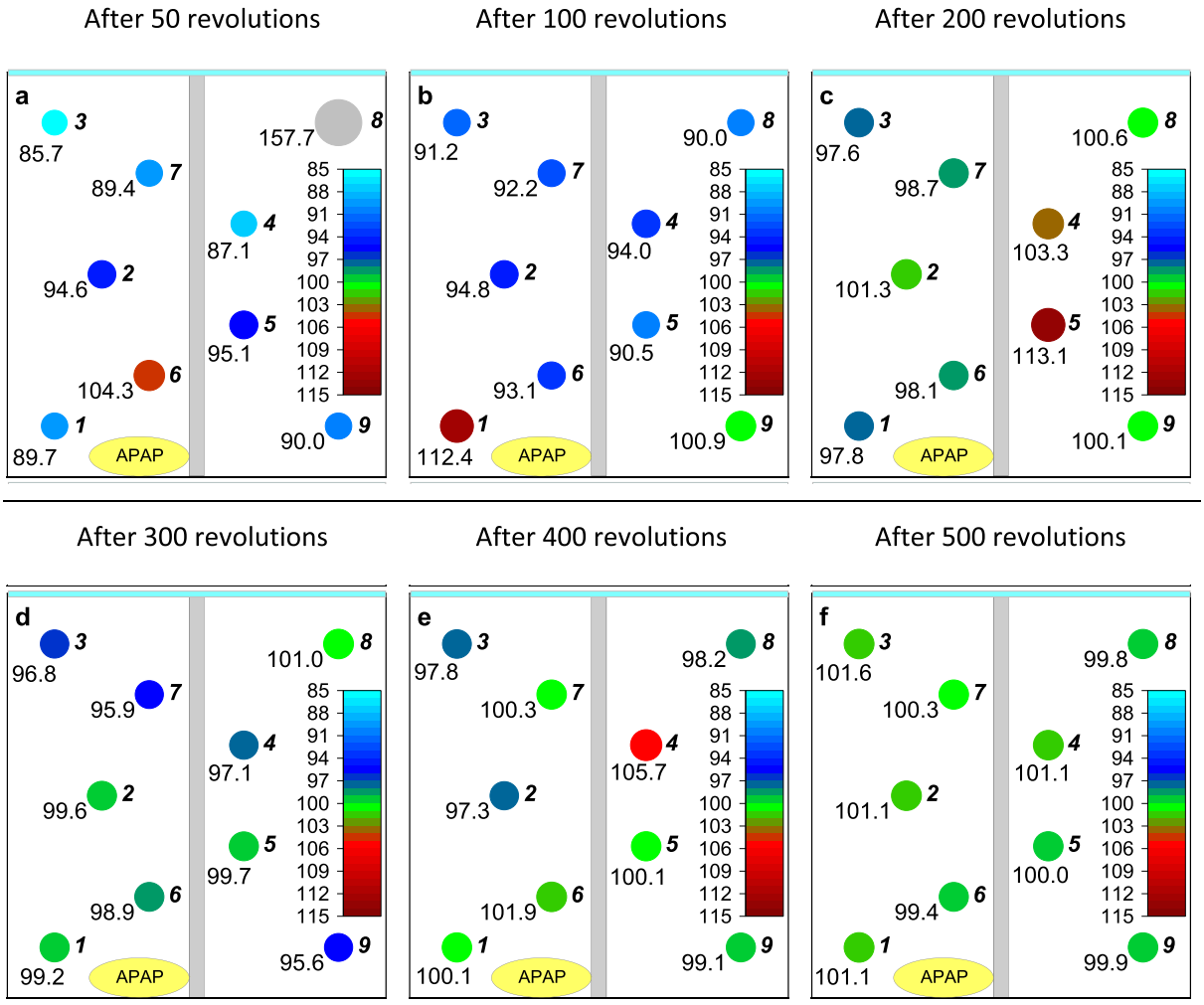

Fig. 13. APAP target content % for blend MB030 at (a) 50 (ca. 261 dm), (b) 100 (ca. 522 dm), (c) 200 (ca. 1044 dm), (d) 300 (ca. 1565 dm), (e) 400 (ca. 2087 dm), and (f) 500 (ca. 2609 dm) revolutions. Values for dm calculated via Eq. (13). Unusual hotspots of API indicated in grey (above 115 % target).

across the entire blend volume, albeit with low homogeneity. This includes areas of both high and low potency. Interestingly, the high concentration of the API is not observed at the original loading position. As blending progresses, represented in the subsequent subfigures in Fig. 13, the concentration appears to level off, eventually reaching around 100 % target for all sampling locations. It also important to note that when there are hotspots present (e.g. locations 6 and 8 in Fig. 13a), these are accompanied by the presence of generalised sub-potent bulk blend (e.g.

locations 1–5, 7, and 9 in Fig. 13a).

Upon examining the APAP content RSD, a similar trend to the ones observed above with the scaled axis is noticeable (Fig. 14a). For three of the blends, several RSD values were inflated beyond the pattern observed by hotspot locations sampled (over 200 % target concentration) however due to lower speed of the run the sampling points are at lower blending extent values relative to Fig. 13 at same number of revolutions and have not reached plateau values. These include 520 % for run MB031, 213 % and 362 % for run MB063, and 437 % and 735 % for run MB064; in the case of the latter (MB064), significantly higher APAP concentration values were recorded for location 8 at 300 revolutions (437 %) and location 6 at 400 revolutions (735 %) (Fig. 16; unusual hotspots indicated in grey). Since the blend MB064 contains only 1 wt% APAP, the sensitivity to changes in concentration is increased compared to blends containing 10 wt%. This is also reflected by the more generalised presence of sub-potent samples with content target % dropping to as low as 47 %.

The removal of hotspot values from the RSD calculation, for visual interpretation purposes, is presented in Fig. 14b. In this case, the data appears to follow the same pattern as seen above for sampling from discharged blend at the end of the blending cycle. This approach could provide an opportunity for reduction in material usage by sampling during blending from fewer blends rather than use individual blends for each set of experimental conditions.

Another way of looking at blending progress is assessing average content, which should reach 100 % target for a uniform blend, as presented in Fig. 15. Similar to the data in Fig. 14, hotspot values (included in Fig. 15a) shift the value of average content significantly; the trend of approaching 100 % target value can be seen clearly. It is interesting to note that two of the blends prepared at 100 RPM (MB063 and MB064) show a progression towards the 100 % value but did not reach it within the experimental space used here, despite the low values of RSD suggesting the lower speed blends have yet to reach a uniform endpoint noting that these mixtures were not run to as high a final blending extent as the 200 RPM batches.

In addition to the trends observed above, considering the API distribution data from Fig. 13 and Fig. 16, a rapid axial and radial distribution of the API is observed. This is the case even at lower extent of mixing that is associated with high RSD values, with API present across the whole Mini Blender volume. The distribution stage seems to be followed by further dispersive mixing, where any API local concentrations or agglomerates are broken up and leading to a homogeneous mixture at length scales comparable with commonly used tablet mass.

3.6. RSD decay fitting

Fitting Eq. (13) to the data (Fig. 17), the regressed parameters listed in Table 6 were obtained with a R^2 value of 0.996. Statistical weighing that applies weight inversely proportional to the value of a datapoint was used due to a higher uncertainty level associated with higher RSD values. It is interesting to note that even though the RSD_{min} fitted value is higher than the estimated best achievable value of 0.4 % for 1 wt% mAPAP blends (Table 5), the value of approx. 2 % is commonly used as an acceptance metric for liquid chromatography measurements, which was used in this study to analyse content uniformity. Application of the RSD decay equation by Palmer and co-workers showed a lower value of RSD_0 [9], however it needs to be noted that in that work the RSD measurements were from tablet assays, and not the blends (whether post-discharge or from within the blender), and as such would be expected to have lower RSD values (from additional mixing within the tablet press feed frame). Additionally, due to using a continuous system, the starting values of strain (related to extent of mixing) used by Palmer and co-workers are higher than the ones used in this study [9], corresponding to starting at higher x-axis values which could influence RSD_0 values.

3.7. Considerations for API physical properties

All the blends above were prepared using micronised APAP grade. However, since API substances can come in a diverse variety of physical forms, it is important to understand the impact of API physical properties on blending performance. For this reason, APAP grades with varying particle size distribution were used in this study, namely, in addition to micronised APAP, in order of increasing particle size: powder, dense powder, special granular, and granular grades (Table 1). API particle size determines the best achievable RSD value for a given sample size (Table 5); observed RSD values for blends prepared with the various physical grades of APAP are plotted against the theoretical RSD limits in Fig. 18. As expected, none of the values are below the parity line, as these would be lower than the theoretical values; data points for each grade are clustered at the same x-axis location as they share the theoretical RSD value.

4. Conclusions

This study used a combination of experimental conditions to explore the blending behaviour of a Gericke GBM 10-P Mini Blender, a semi-continuous blender capable of high-shear, high-RPM mixing

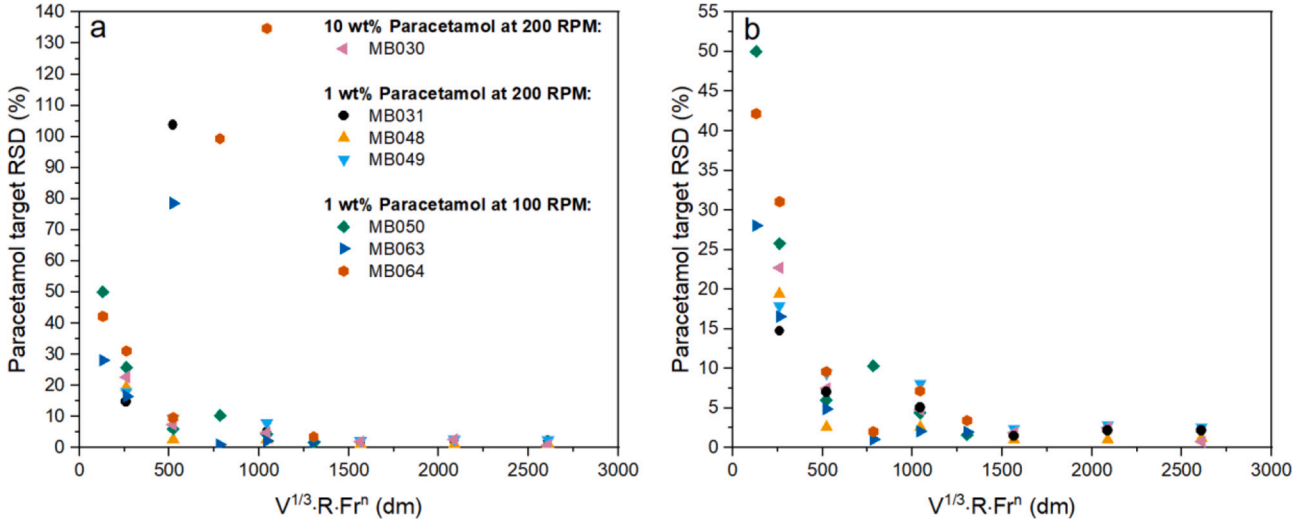

Fig. 14. APAP target RSD for axial dispersion blends plotted against a scaled axis (a) including all data and (b) excluding outlier hotspot values.

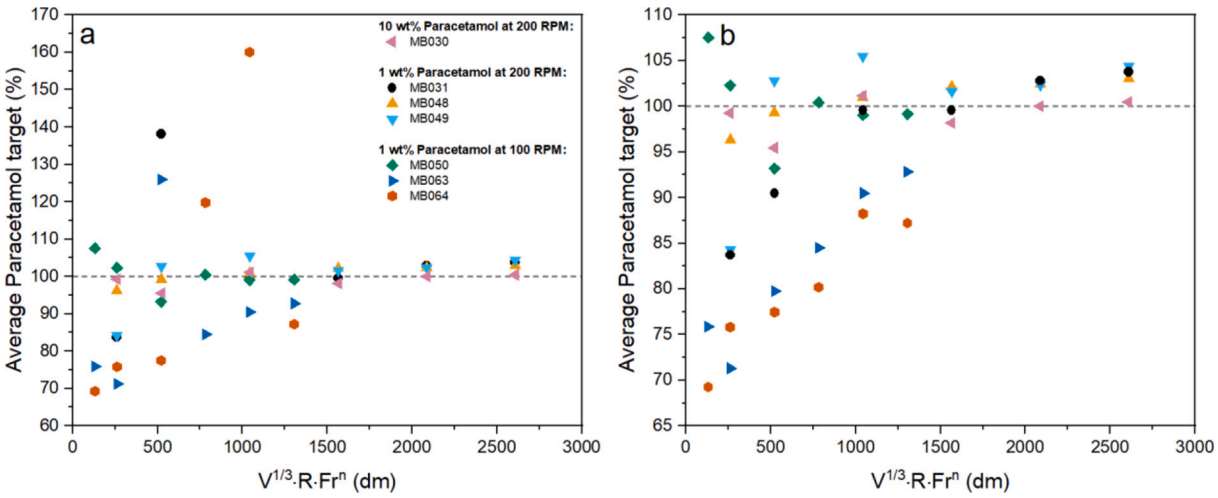

Fig. 15. APAP target content for axial dispersion blends plotted against modified K-M axis (a) including all data and (b) excluding outlier hotspot values.

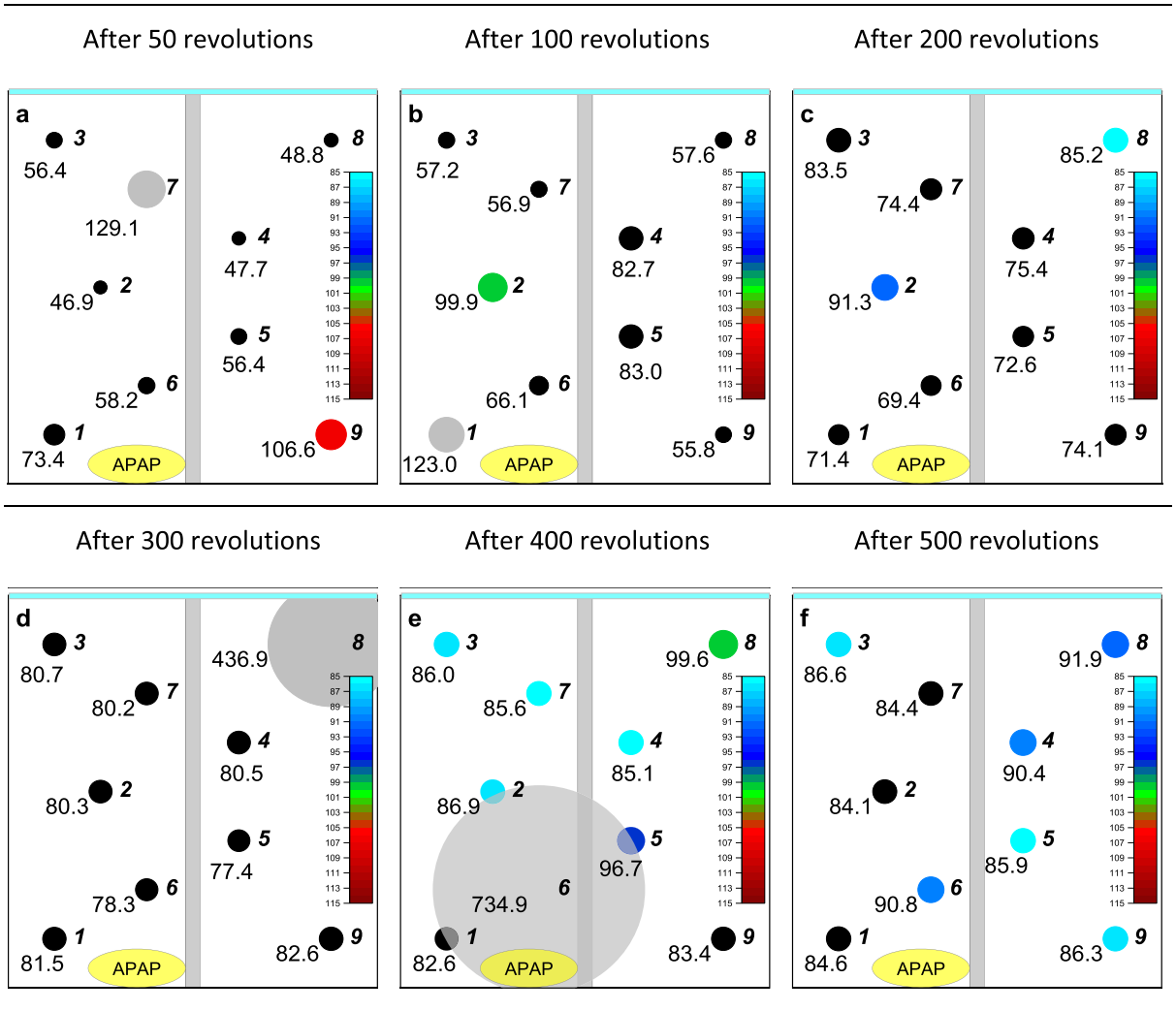

Fig. 16. APAP target content % for blend MB064 at (a) 50 (ca. 130 dm), (b) 100 (ca. 261 dm), (c) 200 (ca. 522 dm), (d) 300 (783 dm), (e) 400 (ca. 1044 dm), and (f) 500 (ca. 1304 dm) revolutions. Values for dm calculated via Eq. (13). Unusual hotspots of API indicated in grey (above 115 % target) and low API content (below 85 % target) indicated in black.

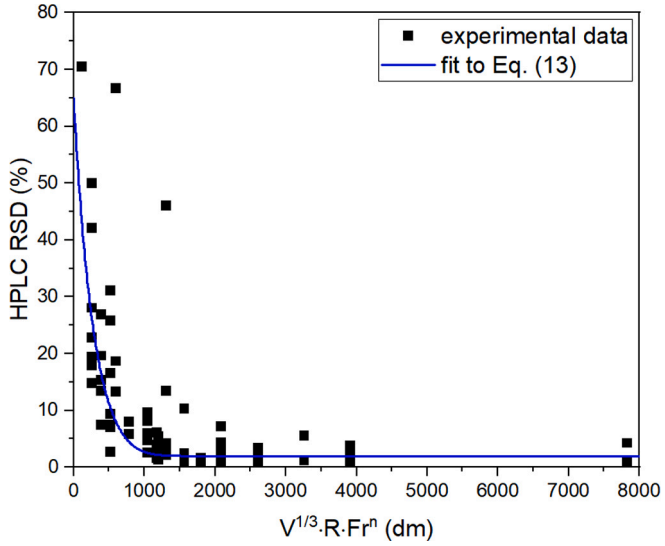

Fig. 17. Fitting of the experimental data to Eq. (13).

Table 6
Regressed Eq. (13) parameters for 1 and 10 wt% mAPAP blends.

Fitting parameter	Obtained value
RSD_{min}	1.98 %
RSD_0	65.0 %
k_b	0.00709 dm^{-1}

conditions. Investigation of a range of blending time and speed values led to scaling of the data with a modified blending extent expression, based on previous lubrication work, collapsing the blend uniformity data across process parameters onto a single curve. This enables comparison with other blending technologies, as well as facilitating the rapid robust definition and optimisation of experimental conditions to obtain either the minimum blend uniformity plateau or a required blend uniformity. The trend of exponentially improving blend RSD to a minimum plateau with this new extent of mixing metric was observed. Reducing the drug content by an order of magnitude resulted in similar trends, showing potential application of this technology in low-dose formulations. A wide range of blender fill levels did not significantly impact blend uniformity, offering an opportunity to use high fill levels for increased production capacity or low fill levels to save material, e.g. during development stages where limited amount of material is available, without compromising product quality. Uniform blends were achieved regardless of the combination of process conditions once sufficiently high blending extent value was reached, even when APAP was placed in a challenging location, allowing flexible selection of process conditions. This offers opportunity to intensify the process for mass throughput via higher shear or fill levels, and the Mini Blender allows the same geometry equipment to be used to address the key needs both in product development and for commercial scale production. Insights from experiments with APAP grades of varying particle size, and physical properties, revealed a blend uniformity limit for each grade related to a representative particle size value ($D_{[6,3]}$), as would be expected for sampling from a random mixture. APAP content RSD values asymptotically reached these limiting values without exceeding the limit, which could be used in define best achievable RSD levels and to compare blending efficiency. The proposed blending extent approach can be used as a useful guide for designing blending process conditions with greater certainty and convenient tool for comparison across blending conditions, scales, and technology types i.e. tumbling or high-shear.

CRediT authorship contribution statement

Martin Prostredny: Writing – review & editing, Writing – original draft, Visualization, Validation, Resources, Methodology, Investigation, Formal analysis, Data curation, Conceptualization. **Hikaru Graeme Jolliffe:** Data curation, Formal analysis, Writing – review & editing. **Richard Elkes:** Writing – review & editing, Supervision, Resources, Methodology, Investigation, Conceptualization. **Khalid Maqsood:** Methodology, Investigation, Conceptualization. **Yunfei Li Song:** Writing – review & editing, Methodology, Investigation, Conceptualization. **Gavin Reynolds:** Writing – review & editing, Conceptualization. **Bernhard Meir:** Writing – review & editing, Methodology. **John Robertson:** Writing – review & editing, Supervision, Resources, Project administration, Investigation, Funding acquisition, Formal analysis, Conceptualization.

Declaration of competing interest

The authors declare the following financial interests/personal relationships which may be considered as potential competing interests:

John Robertson reports financial support and equipment, drugs, or

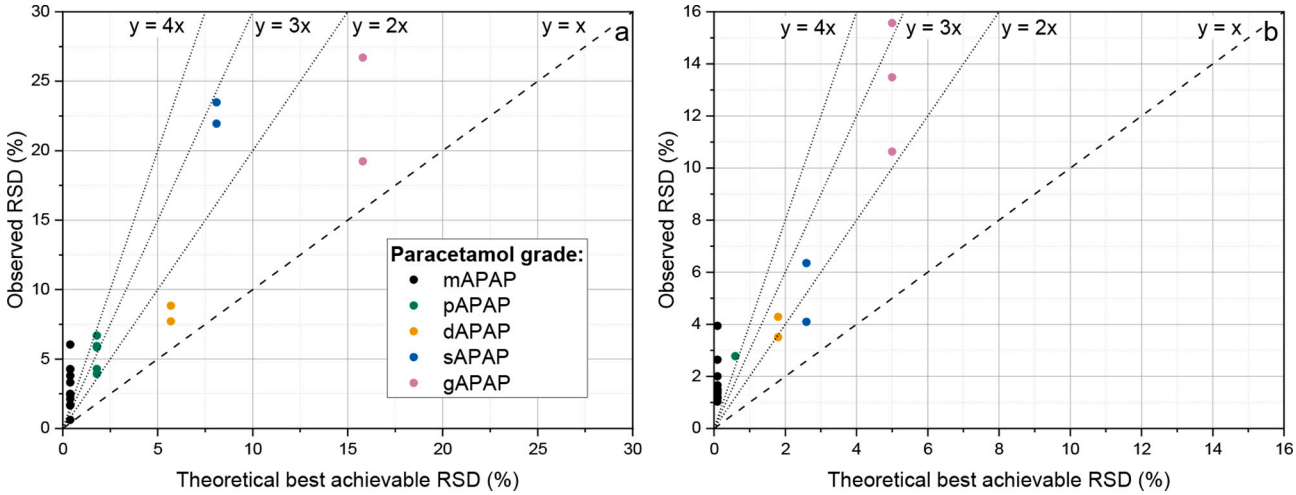

Fig. 18. Observed minimum plateau RSD_{min} versus theoretical best achievable RSD_{ref} for (a) 1 wt% and (b) 10 wt% blends for micronised (mAPAP), powder (pAPAP), dense powder (dAPAP), special granular (sAPAP), and granular (gAPAP) paracetamol with colour physical grade, dotted lines show multiples of theoretical RSD value as visual aid.

supplies were provided by Centre for Process Innovation Limited. John Robertson reports equipment, drugs, or supplies was provided by UK Research and Innovation. If there are other authors, they declare that they have no known competing financial interests or personal relationships that could have appeared to influence the work reported in this paper.

Data availability

Data will be made available on request.

Acknowledgements

This work has been funded by the Medicines Manufacturing Innovation Centre project (MMIC), UK (project ownership: Centre for Process Innovation, CPI). Funding has come from Innovate UK and Scottish Enterprise. Founding industry partners with significant financial and technical support are AstraZeneca and GSK. The University of Strathclyde (via CMAC) is the founding academic partner. Project partners Pfizer and DFE Pharma have provided technical input, data and materials, and project partners Gericke AG have provided technical equipment support and advice. Project partners Siemens and Applied Materials have provided key software and software/IT expertise to other aspects of MMIC GC1 work.

Appendix A. Supplementary data

Supplementary data to this article can be found online at https://doi.org/10.1016/j.powtec.2024.120224.

References

[1] S.L. Lee, T.F. O'Connor, X. Yang, C.N. Cruz, S. Chatterjee, R.D. Madurawe, et al., Modernizing pharmaceutical manufacturing: from batch to continuous production, J. Pharm. Innov. (2015 Mar 19) 1–9.
[2] J. Rantanen, J. Khinast, Wiley.com, 2017 [cited 2024 Jul 11]. Continuous Manufacturing of Pharmaceuticals | Wiley. Available from: https://www.wiley.com/en-ae/Continuous+Manufacturing+of+Pharmaceuticals-p-9781119001324.
[3] I.R. Baxendale, R.D. Braatz, B.K. Hodnett, K.F. Jensen, M.D. Johnson, P. Sharratt, et al., Achieving continuous manufacturing: technologies and approaches for synthesis, workup, and isolation of drug substance. May 20–21, 2014 continuous manufacturing symposium, J. Pharm. Sci. 104 (3) (2015 Mar 1) 781–791.
[4] C.L. Burcham, A.J. Florence, M.D. Johnson, Continuous manufacturing in pharmaceutical process development and manufacturing, Annu. Rev. Chem. Biomol. Eng. 9 (2018 Jun 7) 253–281.
[5] A. Eren, F. Civati, W. Ma, J.C. Gamekkanda, A.S. Myerson, Continuous crystallization and its potential use in drug substance Manufacture: A review, J. Cryst. Growth 601 (2023 Jan 1) 126958.
[6] A. Almaya, L. De Belder, R. Meyer, K. Nagapudi, H.R.H. Lin, I. Leavesley, et al., Control strategies for drug product continuous direct compression—state of control, product collection strategies, and startup/shutdown operations for the production of clinical trial materials and commercial products, J. Pharm. Sci. 106 (4) (2017 Apr 1) 930–943.
[7] D.O. Blackwood, A. Bonnassieux, G. Cogoni, Continuous Direct Compression Using Portable Continuous Miniature Modular & Manufacturing (pcm&m), in: Chemical Engineering in the Pharmaceutical Industry [Internet], John Wiley & Sons, Ltd, 2019, pp. 547–560 [cited 2024 Jul 11]. Available from: https://onlinelibrary.wiley.com/doi/abs/10.1002/9781119600800.ch72.
[8] S. Hurley, A. Tantuccio, M.S. Escotet-Espinoza, M. Flamm, M. Metzger, Development and use of a residence time distribution (RTD) model control strategy for a continuous manufacturing drug product pharmaceutical process, Pharmaceutics 14 (2) (2022 Feb) 355.
[9] J. Palmer, G.K. Reynolds, F. Tahir, I.K. Yadav, E. Meehan, J. Holman, et al., Mapping key process parameters to the performance of a continuous dry powder blender in a continuous direct compression system, Powder Technol. 362 (2020 Feb 15) 659–670.
[10] L. Pernenkil, C.L. Cooney, A review on the continuous blending of powders, Chem. Eng. Sci. 61 (2) (2006 Jan 1) 720–742.
[11] V. Vanhoorne, C. Vervaet, Recent progress in continuous manufacturing of oral solid dosage forms, Int. J. Pharm. (579) (2020 Apr 15) 119194.
[12] S. Mascia, P.L. Heider, H. Zhang, R. Lakerveld, B. Benyahia, P.I. Barton, et al., End-to-end continuous manufacturing of pharmaceuticals: integrated synthesis, purification, and final dosage formation, Angew. Chem. Int. Ed. 52 (47) (2013) 12359–12363.
[13] Fette, Fette Compacting, 2018 [cited 2024 Apr 5]. FE CPS - Continuous Processing System. Available from: https://www.fette-compacting.com/en/products-technologies/continuous-manufacturing/fe-cps.
[14] GEA, Manufacturing medicines for today and the future [Internet], 2016 [cited 2024 Apr 5]. Available from: https://www.gea.com/en/stories/continuous_manufacturing_technologies/.
[15] Gericke, https://www.gerickegroup.com/us/continuousmanufacturing, 2023 [cited 2024 Apr 5]. Continuous Manufacturing. Available from: https://www.gerickegroup.com/us/continuousmanufacturing.
[16] Glatt, Continuous technologies pharma [Internet], 2023 [cited 2024 Apr 5]. Available from: https://www.glatt.com/products/continuous-technologies-pharma/.
[17] Hosokawa Micron, Pharmaceutical Powder Mixing Systems [Internet], 2023 [cited 2024 Apr 5]. Available from: https://www.hosokawa-micron-bv.com/solids-processing/pharmaceutical/pharma-powder-mixing-systems.html.
[18] Lödige, Lödige as partner for the pharmaceutical industry [Internet], 2023 [cited 2024 Apr 5]. Available from: https://www.loedige.de/en/industries/pharmaceuticals/.
[19] J. Wahlich, Review: continuous manufacturing of small molecule solid oral dosage forms, Pharmaceutics 13 (8) (2021 Aug) 1311.
[20] U.S. FDA, Emerging Technology Program Graduates its First Technology. FDA [Internet], 2024 Mar 6 [cited 2024 Jul 11]; Available from: https://www.fda.gov/about-fda/center-drug-evaluation-and-research-cder/news-emerging-technology-program-etp.
[21] M. Leane, K. Pitt, G. Reynolds, A proposal for a drug product Manufacturing Classification System (MCS) for oral solid dosage forms, Pharm. Dev. Technol. 20 (1) (2015 Jan 2) 12–21.
[22] S. Byrn, M. Futran, H. Thomas, E. Jayjock, N. Maron, R.F. Meyer, et al., Achieving continuous manufacturing for final dosage formation: challenges and how to meet them May 20–21 2014 Continuous manufacturing symposium, J. Pharm. Sci. 104 (3) (2015 Mar 1) 792–802.
[23] A.U. Vanarase, F.J. Muzzio, Effect of operating conditions and design parameters in a continuous powder mixer, Powder Technol. 208 (1) (2011 Mar 10) 26–36.
[24] W. Yang, S. Krull, N. Pavurala, X. Xu, T. O'Connor, G. Tian, Assessing residence time distributions and hold-up mass in continuous powder blending using discrete element method, Chem. Eng. Res. Des. 190 (2023 Feb 1) 10–19.
[25] P.H.M. Janssen, S. Fathollahi, B. Bekaert, D. Vanderroost, T. Roelofs, V. Vanhoorne, et al., Impact of material properties and process parameters on tablet quality in a continuous direct compression line, Powder Technol. 424 (2023 Jun 15) 118520.
[26] U.S. FDA, Q13 Continuous Manufacturing of Drug Substances and Drug Products [Internet]. FDA, 2023 [cited 2024 Jul 11]. Available from: https://www.fda.gov/regulatory-information/search-fda-guidance-documents/q13-continuous-manufacturing-drug-substances-and-drug-products.
[27] M. Jaspers, T.P. Roelofs, A. Lohrmann, F. Tegel, M.K. Maqsood, Y.L. Song, et al., Process intensification using a semi-continuous mini-blender to support continuous direct compression processing, Powder Technol. 428 (2023 Oct 1) 118844.
[28] Y. Gao, F.J. Muzzio, M.G. Ierapetritou, Optimizing continuous powder mixing processes using periodic section modeling, Chem. Eng. Sci. 80 (2012 Oct 1) 70–80.
[29] J. Kushner, Incorporating Turbula mixers into a blending scale-up model for evaluating the effect of magnesium stearate on tablet tensile strength and bulk specific volume, Int. J. Pharm. 429 (1) (2012 Jun 15) 1–11.
[30] J. Kushner, F. Moore, Scale-up model describing the impact of lubrication on tablet tensile strength, Int. J. Pharm. 399 (1) (2010 Oct 31) 19–30.
[31] J. Kushner, H. Schlack, Commercial scale validation of a process scale-up model for lubricant blending of pharmaceutical powders, Int. J. Pharm. 475 (1) (2014 Nov 20) 147–155.
[32] H.G. Jolliffe, M. Prostredny, C. Mendez Torrecillas, E. Bordos, C. Tierney, E. Ojo, et al., A modified Kushner-Moore approach to characterising small-scale blender performance impact on tablet compaction, Int. J. Pharm. 659 (2024 Jun 25) 124232.
[33] D. Brone, A. Alexander, F.J. Muzzio, Quantitative characterization of mixing of dry powders in V-blenders, AICHE J. 44 (2) (1998) 271–278.
[34] J. Hilden, M. Schrad, J. Kuehne-Willmore, J. Sloan, A first-principles model for prediction of product dose uniformity based on drug substance particle size distribution, J. Pharm. Sci. 101 (7) (2012 Jul) 2364–2371.